

RESEARCH

Open Access



EIF4A3-regulated circ_0087429 can reverse EMT and inhibit the progression of cervical cancer via miR-5003-3p-dependent upregulation of OGN expression

Meiqin Yang^{1†}, Haoran Hu^{1†}, Sufang Wu^{2†}, Jianyi Ding¹, Bo Yin¹, Baoyou Huang³, Fang Li^{4*}, Xiaoqing Guo^{1*} and Lingfei Han^{1*}

Abstract

Background: Circular RNAs (circRNAs) are noncoding RNAs with stable structures with high expression and tissue-specific expression. Studies have shown that circRNA dysregulation is closely related to the progression of tumours. However, the function and regulatory mechanism of most circRNAs in cervical cancer are still unclear.

Methods: CircRNAs related to cervical cancer were screened through the Gene Expression Omnibus (GEO) database. qRT-PCR was used to verify the expression of circ_0087429 in cervical cancer tissues and cells. Then, in vivo and in vitro experiments were conducted to evaluate the role of circ_0087429 in the progression of cervical cancer. The role of the circ_0087429/miR-5003-3p/osteoglycin (OGN) axis in the epithelial to mesenchymal transition (EMT) was confirmed by rescue experiments, fluorescence in situ hybridization, luciferase reporter assays, immunofluorescence staining and western blotting. The inhibitory effect of Eukaryotic initiation factor 4A-III (EIF4A3) on the biogenesis of circ_0087429 was verified by RNA immunoprecipitation (RIP) assays and qRT-PCR.

Results: circ_0087429 is significantly downregulated in cervical cancer tissues and cells and negatively correlated with International Federation of Gynecology and Obstetrics (FIGO) staging and lymphatic metastasis in cervical cancer patients. circ_0087429 can significantly inhibit the proliferation, migration, invasion and angiogenesis of cervical cancer in vitro and tumour growth and metastasis in vivo. OGN is significantly downregulated in cervical cancer tissues and cells. circ_0087429 can upregulate the expression of OGN by competitively binding with miR-5003-3p, thereby reversing EMT and inhibiting the progression of cervical cancer. EIF4A3 can inhibit circ_0087429 expression by binding to its flanking regions.

*Correspondence: fang_li@tongji.edu.cn; guoxiaoqing@51mch.com; lingfeihan@126.com

[†]Meiqin Yang, Haoran Hu and Sufang Wu contributed equally to this work.

¹ Department of Gynecology, Shanghai First Maternity and Infant Hospital, School of Medicine, Tongji University, Shanghai 200092, China

⁴ Department of Gynecology, Shanghai East Hospital, School of Medicine, Tongji University, Shanghai 200120, China

Full list of author information is available at the end of the article



© The Author(s) 2022. **Open Access** This article is licensed under a Creative Commons Attribution 4.0 International License, which permits use, sharing, adaptation, distribution and reproduction in any medium or format, as long as you give appropriate credit to the original author(s) and the source, provide a link to the Creative Commons licence, and indicate if changes were made. The images or other third party material in this article are included in the article's Creative Commons licence, unless indicated otherwise in a credit line to the material. If material is not included in the article's Creative Commons licence and your intended use is not permitted by statutory regulation or exceeds the permitted use, you will need to obtain permission directly from the copyright holder. To view a copy of this licence, visit <http://creativecommons.org/licenses/by/4.0/>. The Creative Commons Public Domain Dedication waiver (<http://creativecommons.org/publicdomain/zero/1.0/>) applies to the data made available in this article, unless otherwise stated in a credit line to the data.

Conclusions: As a tumour suppressor, circ_0087429 regulated by EIF4A3 can reverse EMT and inhibit the progression of cervical cancer through the miR-5003-3p/OGN axis. It is expected to become a potential target for the treatment of cervical cancer.

Keywords: Circ_0087429, Cervical cancer, MiR-5003-3p, OGN, Epithelial to mesenchymal transition, EIF4A3

Introduction

Cervical cancer is the fourth most common cancer in the world and poses a serious threat to women's health [1]. Due to the increase in human papilloma virus (HPV) infections and the confusion regarding screening procedures, the incidence and mortality of cervical cancer have increased, while the age of onset has decreased [2]. A preventive vaccine for cervical cancer is currently on the market, but it is not effective for women with cervical precancerous lesions or cervical cancer [3]. Therefore, it is particularly important to further explore the molecular mechanism of the occurrence and development of cervical cancer and to actively screen for possible new specific molecular targets for the treatment of cervical cancer.

Circular RNA (circRNA) is a type of noncoding RNA with a closed-loop structure. Its structure is stable and not easily degraded by exonuclease due to the absence of 5' caps and 3' tails [4]. With the advancement of gene sequencing and bioinformatics technology in recent years, a large number of circRNAs have been found to be involved in various biological processes, such as cancer proliferation, migration, invasion and drug resistance [5, 6]. The mechanism of action of circRNA is also complex and diverse. CircRNAs can be used as scaffolds for the assembly of protein complexes [7]; circRNAs can regulate gene transcription and RNA splicing [8]; circRNAs containing internal ribosome entry site elements and open reading frames can also be translated into proteins or polypeptides [9]. However, the most common mechanism of action of circRNA in cancer is the competitive endogenous RNA (ceRNA) mechanism. Studies have found that most circRNA sequences contain miRNA binding sites, which allow them to interact with miRNAs. This interaction prevents the binding of miRNA and mRNA, and thus, a circRNA-miRNA-mRNA functional network is formed [10]. For example, in pancreatic ductal adenocarcinoma, circEYA3 induces energy production through the miR-1294/c-Myc axis to promote tumour progression [11]; circCCDC9 can regulate the expression of CAV1 by adsorbing miR-6792-3p to inhibit the occurrence and development of gastric cancer [12]. In cervical cancer, the role of some circRNAs, such as circTPCN [13] and circZFR [14], has been reported. However, the functions of most circRNAs have not yet been elucidated.

MicroRNAs (miRNAs) are endogenous short-stranded noncoding RNAs of nearly 20 nucleotides. They can

inhibit translation and promote mRNA degradation [15]. The abnormal regulation of miRNA is closely related to tumorigenesis. Changes in miRNA expression can induce a series of cascading reactions and feedback pathways [16]. The role and related pathways of miR-5003-3p have not been well reported. Only Kwak et al.'s studies have shown that miR-5003-3p in breast cancer can promote the stability of snail by targeting E-cadherin and MDM2 and then promote the metastasis of breast cancer through the epithelial to mesenchymal transition (EMT) pathway [17]. There is no report on the role of miR-5003-3p in cervical cancer.

Small leucine-rich proteoglycans (SLRPs) are secreted by a variety of cells, are mainly located in the extracellular matrix, and can participate in various biological processes, such as signal transduction, cell adhesion, and DNA repair [18, 19]. Osteoglycin (OGN) is a type of SLRP that has been found to be downregulated in many different cancers, including cervical cancer, breast cancer, and colon cancer [20–22]. The specific role and regulatory mechanism of OGN in cervical cancer are still unknown.

In this study, we first discovered that circ_0087429 was significantly downregulated in cervical cancer. Subsequently, its clinical significance in cervical cancer was discussed, and its effect and regulatory mechanism were studied through in vivo and in vitro experiments. circ_0087429 can be used as a molecular sponge of miR-5003-3p to reverse EMT by regulating the expression of the target gene OGN, thereby inhibiting the occurrence and development of cervical cancer. EIF4A3 can inhibit the biogenesis of circ_0087429. This research provides a potential target for the pathogenesis and treatment of cervical cancer.

Materials and methods

Patient tissue samples and cell lines

This study included 44 patients with cervical cancer who were treated at the Shanghai First Maternity and Infant Hospital from January to December 2017. None of the patients received chemotherapy or radiotherapy before biopsy or surgery. After surgical resection, samples of cervical cancer tissues and matched adjacent tissues were immediately frozen in liquid nitrogen and then transferred to a -80 °C refrigerator for stable storage until use. This study was approved by the Ethics Committee of the

Shanghai First Maternity and Infant Hospital. All the included patients signed informed consent forms. The histopathological and clinical data came from pathology reports and medical records.

A human cervical immortalized squamous cell line (Ect1/E6E7) and human cervical cancer cell lines (HeLa, SiHa and CaSki) were provided by the American Type Culture Collection (ATCC, USA). DMEM (Gibco, USA) was used to cultivate HeLa and SiHa cells, and RPMI-1640 medium (Gibco, USA) was used to cultivate CaSki cells. Ten percent foetal bovine serum (Gibco, USA) was added to the above two types of media. Ect1/E6E7 cells were cultured in keratinocyte serum-free medium with 0.1 ng/ml human recombinant EGF, 0.05 mg/ml bovine pituitary extract and 44.1 mg/L calcium chloride. All cell lines were cultured at 37 °C in a humidified incubator containing 5% CO².

Quantitative real-time polymerase reaction (qRT-PCR)

TRIzol reagent was used to extract total RNA from the tissue or cell line according to the manufacturer's instructions. For circRNA and mRNA, the PrimeScript RT reagent Kit (Takara, Japan) was used to synthesize total RNA into cDNA, and TB Green Premix Ex Taq II (Takara, Japan) was used for cDNA amplification. For miRNA, the microRNA Reverse Transcription Kit (EZBioscience, USA) was used for reverse transcription, and Probe qPCR Master Mix for microRNA (EZBioscience, USA) was used for cDNA expansion. β -Actin, GAPDH and U6 were used as internal controls. The expression of each gene was normalized to that of the internal control and quantified using the 2^{- $\Delta\Delta$ CT} method. Related primer sequences are shown in Additional file 1: Table S1.

Cell transfection and stable transfection strain construction

Circ_0087429 was overexpressed by pcDNA5.1-ciR integrated with the full-length sequence of circ_0087429 (Genesee, China). OGN and EIF4A3 was overexpressed by PGMLV-6395 integrated with the full-length sequence of OGN or EIF4A3 (Genomeditech, China). According to the manufacturer's protocol, Lipofectamine 3000 Reagent (Thermo Fisher Scientific, USA) was used for transfection. After successful transfection, cell lines were screened with 2 μ g/ml puromycin for 30 days. In addition, the silencing of circ_0087429, OGN and EIF4A3 were achieved by si-circ_0087429, si-OGN and si-EIF4A3 respectively, and si-NC was a negative control. The overexpression and inhibition of miR-5003-3p were achieved by miR-5003-3p mimics and miR-5003-3p inhibitors, and NC mimics and NC inhibitors were used as controls (provided by Genomeditech, China). The above

oligonucleotide sequences are shown in Additional file 1: Table S2.

RNase R treatment

Two micrograms of total RNA with or without 5 U/ μ g RNase R (Epicentre Technologies, USA) was incubated at 37 °C for 30 min. Then, qRT-PCR was used to detect the expression of circ_0087429 and the parental gene SPIN1.

Actinomycin D assays

Cells were seeded in six-well plates (4 \times 10⁵ cells per well). Twenty-four hours later, 2 μ g/ml actinomycin D (Sigma, USA) was added to the cells. Then, total RNA was collected at the specified time, and the expression of circ_0087429 and SPIN1 was detected by qRT-PCR. The half-life was the time required for the RNA level to reach 50% of that at 0 h.

Nucleocytoplasmic fractionation

Separation of cytoplasmic and nuclear RNA in SiHa and HeLa cells was carried out using the Cytoplasmic and Nuclear RNA Purification Kit (Norgenbiotek Corporation, Canada). qRT-PCR was used to detect the relative expression levels of circ_0087429 and SPIN1. U6 was used as the internal reference for the nuclear fraction, and GAPDH was used as that for the cytoplasmic fraction.

Fluorescence in situ hybridization (FISH)

FAM-labelled circ_0087429 and Cy3-labelled miR-5003-3p were used to observe the cellular localization of the two. According to the manufacturer's instructions, circ_0087429 and miR-5003-3p probes were used for hybridization overnight, and then the nuclei were counterstained with DAPI. The pictures were acquired by a Zeiss LSM710 laser scanning confocal microscope (Zeiss Instrument Inc., Germany).

Cell Counting Kit-8 (CCK-8) assay

CCK-8 reagent (Dojindo, Japan) was used to evaluate the proliferation ability of cervical cancer cells. Cells were seeded in 96-well plates at 1 \times 10³ cells per well. After culturing for 0, 24, 48, 72, and 96 h, CCK-8 solution (10 μ L) was added to each well, incubated for 2 h in an incubator, and then a spectrophotometer was used to evaluate the absorbance at 450 nm.

5-Ethynyl-20-deoxyuridine (EdU) Assay

The Cell-Light EdU DNA cell proliferation kit (RiboBio, China) was used for EdU detection. Cells were incubated with EdU for 2 h and then fixed with 4% paraformaldehyde, followed by dyeing and sealing with Apollo dye solution and Hoechst 33,342. An inverted fluorescence

microscope (Carl Zeiss, Germany) was used to take pictures to evaluate the proportion of EdU-positive cells.

Colony formation assay

The cells to be tested were seeded in a 6-well plate at 800 cells per well. After 2 weeks of culture, the cells were fixed with 4% paraformaldehyde for 15 min and stained with 0.5% crystal violet solution for 15 min. Finally, the colonies were counted.

Wound healing assay

The cells were cultured in a 6-well plate to 90% confluence. A 200- μ l pipette tip was used to create a scratch of the same width. A microscope was used to acquire images immediately. The cells were then incubated in serum-free medium for 24 h and 48 h and photographed again. The wound width was recorded at each time point.

Transwell invasion assay

The transwell chamber (Corning, USA) was paved with matrigel mix (BD Biosciences, USA) for invasion assays. According to the manufacturer's protocol, 200 μ l of the cell suspension was placed in serum-free medium in the upper chamber, and 20% FBS medium was added to the lower chamber. After 24 h of incubation, cotton swabs were used to remove the cells inside the upper chamber. The cells that invaded the bottom of the membrane were fixed and stained. A microscope was used to take pictures and then evaluate the number of cells with ImageJ software.

Tube formation assay

HUVECs were plated in 96-well plates coated with Matrigel (Corning, USA) at a density of 4×10^4 cells per well. After incubating for 3–4 h in the incubator, calcein AM (Sigma, USA) was added to the plate. A fluorescence microscope (Carl Zeiss, Germany) was used to take pictures and then analyse the tube-forming ability of each group of cells.

Western blotting

One percent PMSF added to RIPA lysis buffer (Beyotime, China) was used to extract total proteins. The same amounts of protein were separated by 10% SDS-PAGE, transferred to PVDF membranes (Millipore, USA), and then sealed with skim milk. The blots were incubated with the primary antibody at 4 °C for 12 h and then with the secondary antibody at room temperature for 1 h. An electrochemiluminescence kit (Millipore, USA) was used for the visualization of protein signals. β -Actin was the internal control. Primary antibodies were anti-E-cadherin, anti-N-cadherin, anti-Claudin-1, anti-Vimentin,

anti-Snail, anti-OGN, anti-MMP2 and anti-EIF4A3 from Abcam (Cambridge, UK).

Luciferase reporter assay

The sequences that bind to miR-5003-3p in the circ_0087429 region and the OGN-3'UTR and their corresponding mutant sequences were synthesized and inserted into the luciferase reporter vector GM-1013FL02 and named circ_0087429-WT, circ_0087429-MUT, OGN-WT and OGN-MUT, respectively (Genomeditech, China). These plasmids were cotransfected with miR-5003-3p mimics or mimics NC. Then, according to the manufacturer's protocol, the relative luciferase activity was checked with the Pierce Renilla-Firefly Luciferase Dual Assay Kit (Thermo Fisher Scientific, USA).

Cell immunofluorescence (IF) staining

A 4% formaldehyde solution was used to fix the cells for 15 min. Triton X-100 (0.2%) was used to permeabilize the cell membrane for 30 min. Then, the cells were blocked in blocking solution at room temperature for 1 h, and the primary antibodies were added and incubated overnight at 4 °C. Then, the fluorophore-tagged secondary antibodies were incubated for 1 h at room temperature. After that, the nuclei were counterstained with DAPI for 15 min and photographed with a confocal microscope.

RNA immunoprecipitation (RIP) assay

RIP assay was performed using an EZMagna RIP kit (Millipore, USA) according to the manufacturer's protocol. The magnetic beads were incubated with anti-EIF4A3 antibody or IgG negative control antibody. Cell lysates were then incubated with the corresponding antibody-coated beads. Finally, the immunoprecipitated RNA was extracted and detected by qRT-PCR.

Immunohistochemistry (IHC) examination

Tissue sections were deparaffinized with xylene and dehydrated with a graded alcohol series. Afterwards, the slices were treated with 3% hydrogen peroxide and pressure-cooked for antigen retrieval. Then, the slices were incubated with anti-OGN, anti-E-cadherin, anti-N-cadherin, anti-CD31 and anti-Ki67 primary antibodies from Abcam (Cambridge, UK) at 4 °C overnight and then incubated with the appropriate secondary antibodies for 1 h at room temperature. Finally, the sections were treated with 3'-diaminobenzidine tetrahydrochloride and counterstained with haematoxylin.

Xenograft assay

All animal care and experiments were conducted in accordance with the guidelines of the National Institutes

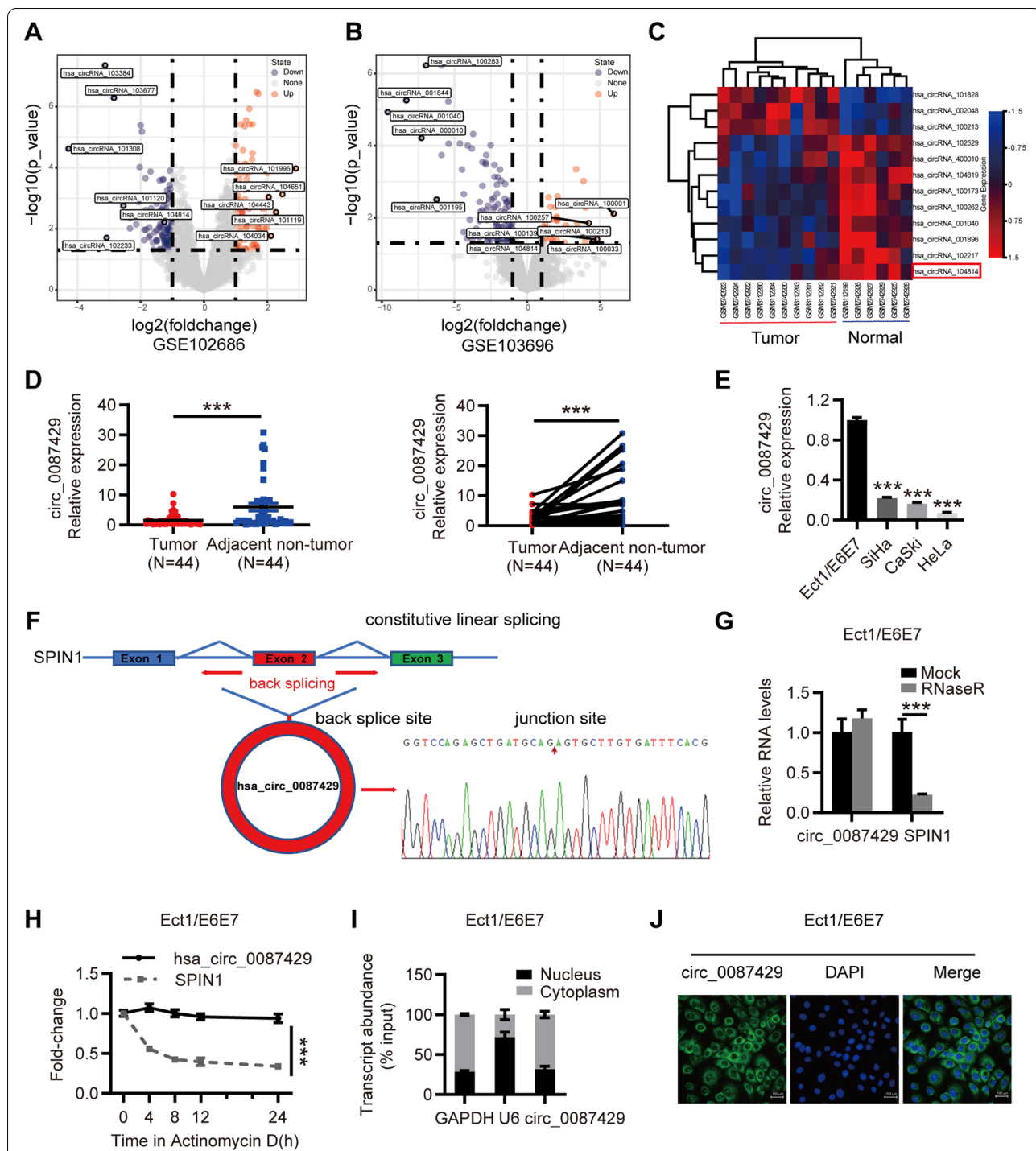


Fig. 1 The expression and characteristics of circ_0087429 in cervical cancer. **a.** Differentially expressed circRNAs between cervical cancer and adjacent tissue samples in the GSE102686 dataset. **b.** Differentially expressed circRNAs between cervical cancer and normal cervical epithelial cell lines in the GSE103696 dataset. **c.** Heatmap of circRNAs with significant differential expression in two datasets (GSE102686 and GSE103696). circ_0087429 (hsa_circRNA_104814) is marked with a red box. **d.** Differential expression of circ_0087429 in 44 pairs of cervical cancer and adjacent tissue samples. **e.** Differential expression of circ_0087429 between cervical cancer and normal cervical epithelial cell lines. **f.** The Sanger sequencing results showed that circ_0087429 was formed by head-to-tail splicing of the second exon of the parental gene SPIN1. **g.** The expression of circ_0087429 and SPIN1 after RNaseR treatment was detected by qRT-PCR. **h.** The expression changes in circ_0087429 and SPIN1 at different time points after adding actinomycin D were determined by qRT-PCR. **i.** A subcellular fractionation assay was used to detect the relative expression of circ_0087429 in the cytoplasm and nucleus. U6 was used as the internal reference for the nuclear fraction, and GAPDH was used as that for the cytoplasmic fraction. **j.** FISH staining confirmed the expression of circ_0087429 in the cytoplasm. Scale bar, 100 μ m. *** p < 0.001

Table 1 Correlations between the expression of circ_0087429 and OGN and clinicopathological parameters of cervical cancer patients

Characteristics	Cases	circ_0087429 expression			OGN expression		
		Low(22)	High(22)	<i>p</i>	Low(22)	High(22)	<i>p</i>
Age (years)				0.531			0.531
< 45	16	9	7		9	7	
≥ 45	28	13	15		13	15	
FIGO stage				0.042*			0.176
Ib	32	13	19		14	18	
IIa-IIb	12	9	3		8	4	
Tumour size(cm)				0.099			0.003*
< 4	31	13	18		11	20	
≥ 4	13	9	4		11	2	
Lymph node invasion				0.031*			0.150
Absent	34	14	20		15	19	
Present	10	8	2		7	3	
Stromal invasion				0.099			0.741
< 1/2	13	4	9		6	7	
≥ 1/2	31	18	13		16	15	

FIGO International Federation of Gynecology and Obstetrics; * *P* < 0.05

of Health and approved by the Animal Care Committee of Tongji University. We chose 4-week-old female BALB/c nude mice for tumour xenografts experiments. In tumour growth assay in vivo, HeLa cells stably transfected with pcDNA5.1-NC or pcDNA5.1-circ_0087429 were injected subcutaneously into the upper back of nude mice (1×10^7 , 100 μ l). The size of the tumours was measured with a calliper every week. The tumour volume was calculated as length \times width² \times 0.5. Twenty-eight days after the injection, the mice were euthanized, and the tumours were dissected for further analysis. In tumour metastasis assay in vivo, HeLa cells stably transfected with pcDNA5.1-NC or pcDNA5.1-circ_0087429 were injected into nude mice through the tail vein (5×10^6 , 150 μ l). After five weeks, the mice were euthanized, and the livers and lungs were dissected, embedded in paraffin, and finally validated by haematoxylin and eosin (H&E) staining.

Statistical analysis

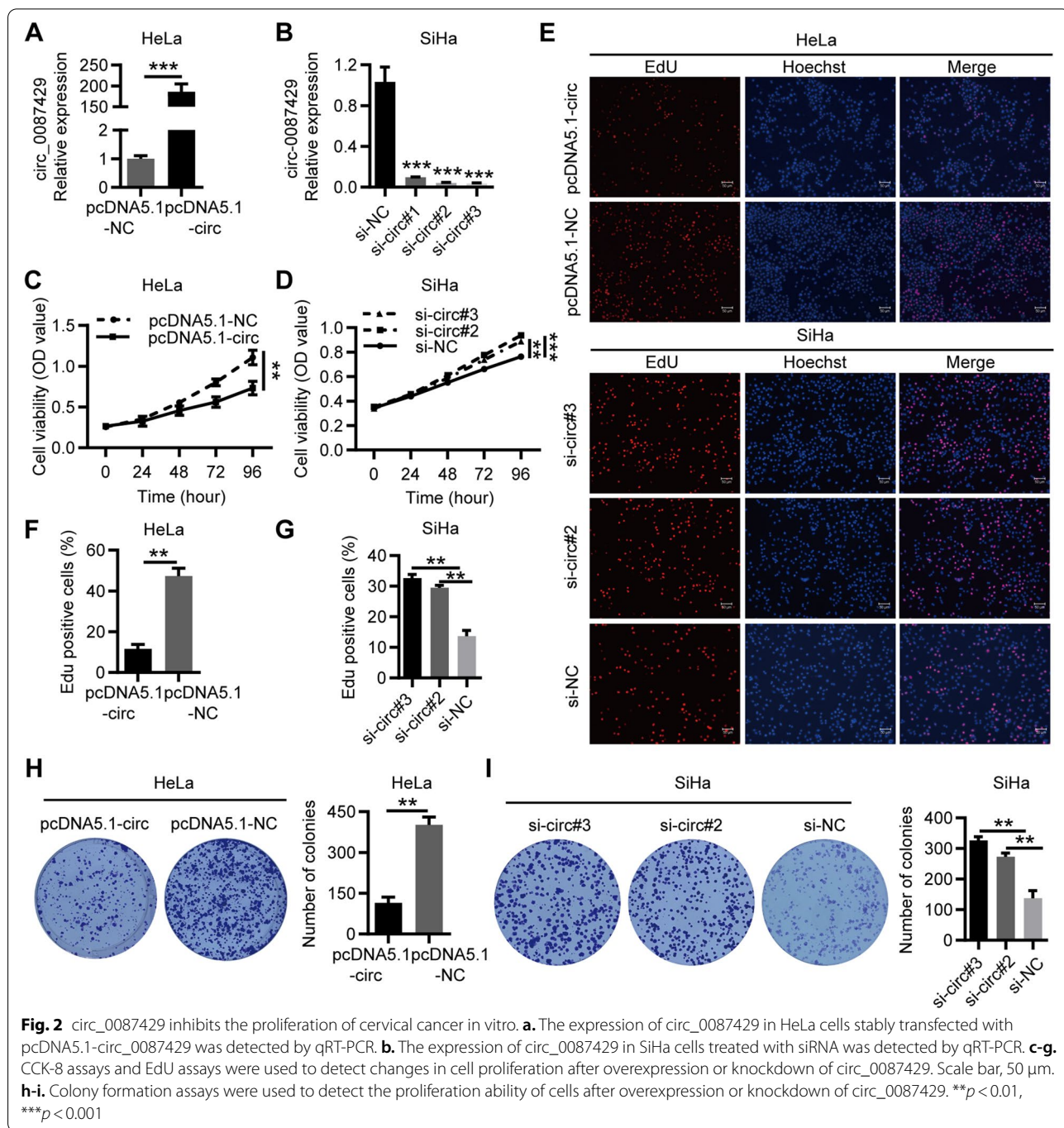
Statistical analyses were performed using SPSS 22.0 (IBM, SPSS, Chicago, USA) and GraphPad Prism 9.1.0 (GraphPad, La Jolla, CA, USA). Student’s t test (two-tailed) was used to compare the differences between the two groups, and one-way ANOVA was used to compare the differences among multiple groups. Pearson correlation analysis was used to analyse the correlations. The results of quantitative data are expressed as the mean \pm SD. All experiments were repeated at least 3

times. For all the above analysis results, *p* < 0.05 was considered to indicate a significant difference.

Results

The expression and clinical significance of circ_0087429 in cervical cancer

First, we screened the differentially expressed circRNAs between cervical cancer and normal cervical samples in circRNA microarray datasets in the Gene Expression Omnibus (GEO) database. The GSE102686 dataset contained 5 pairs of cervical cancer and adjacent tissue samples, and the GSE113696 dataset contained 1 normal cervical epithelial cell line, HcerEpic, and 5 cervical cancer cell lines, HeLa, CaSki, SiHa, C-33A, SW756. Both groups of microarray datasets showed that hsa_circRNA_104814 (hsa_circ_0087429) was downregulated by more than onefold in cervical cancer versus adjacent tissues (Fig. 1a-c). To further verify this expression difference, we collected 44 pairs of cervical cancer and adjacent tissue samples. The qRT-PCR results showed that circ_0087429 was significantly downregulated in cervical cancer tissues, which was consistent with the microarray results (Fig. 1d). The relationship between circ_0087429 and the clinicopathological parameters of cervical cancer patients is shown in Table 1. Compared with that in stage I cervical cancer patients, the expression of circ_0087429 in stage II patients was significantly reduced; the expression of circ_0087429 was reduced in patients with



(See figure on next page.)

Fig. 3 circ_0087429 inhibits migration, invasion and angiogenesis of cervical cancer in vitro. **a-b.** Wound healing assays determined the migration ability of cells after overexpression or knockdown of circ_0087429. Scale bar, 100 μ m. **c-d.** Transwell invasion assays detected the invasion ability of cells after overexpression or knockdown of circ_0087429. Scale bar, 50 μ m. **e-f.** After HUVECs were cocultured with circ_0087429-overexpressing or circ_0087429-knockdown cells, the tube-forming ability was detected. Scale bar, 50 μ m. **g.** The expression of circ_0087429 in HUVECs after coculture with circ_0087429 overexpression or knockdown cells was detected by qRT-PCR. ** $p < 0.01$, *** $p < 0.001$

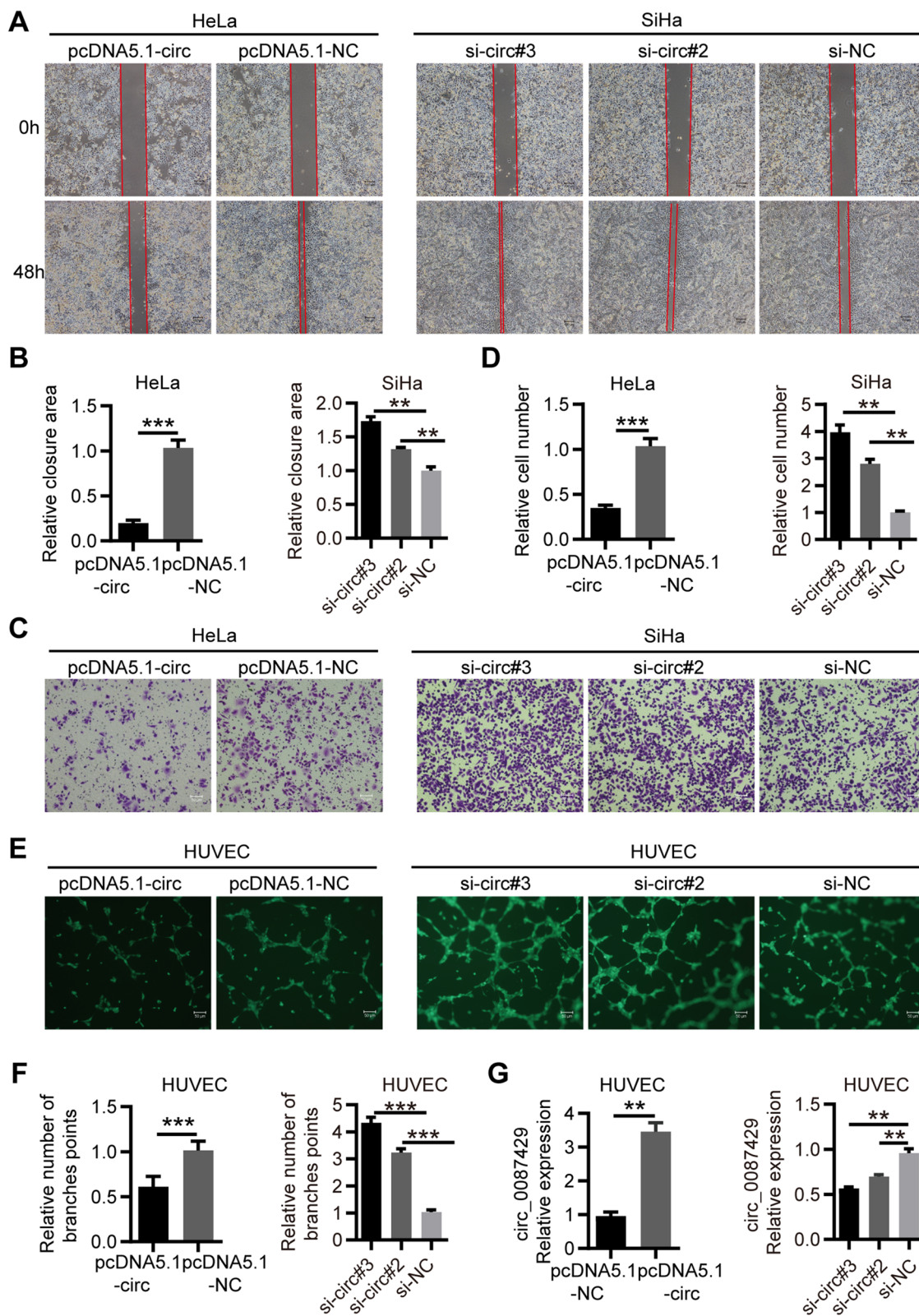


Fig. 3 (See legend on previous page.)

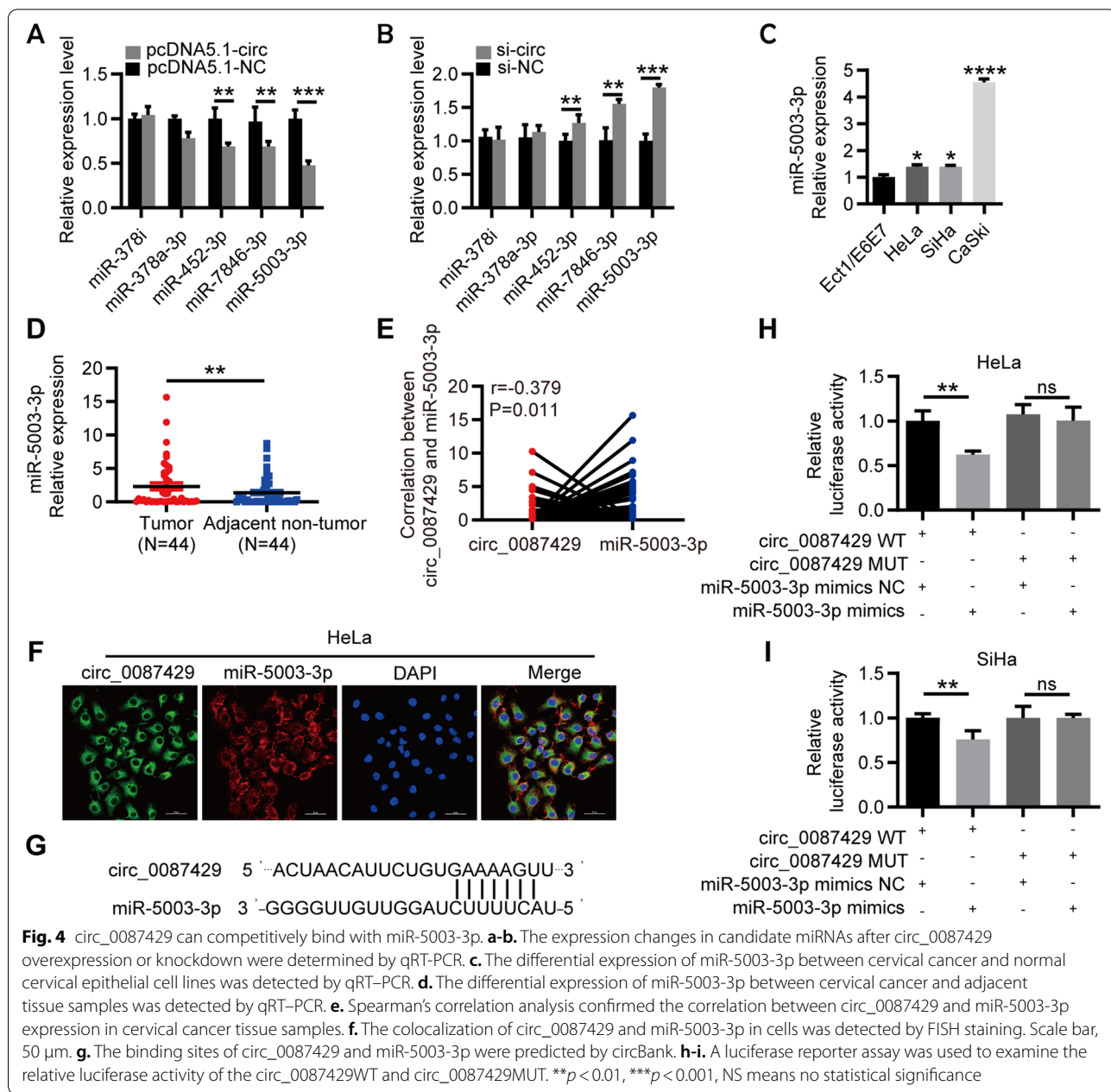


Fig. 4 circ_0087429 can competitively bind with miR-5003-3p. **a-b.** The expression changes in candidate miRNAs after circ_0087429 overexpression or knockdown were determined by qRT-PCR. **c.** The differential expression of miR-5003-3p between cervical cancer and normal cervical epithelial cell lines was detected by qRT-PCR. **d.** The differential expression of miR-5003-3p between cervical cancer and adjacent tissue samples was detected by qRT-PCR. **e.** Spearman's correlation analysis confirmed the correlation between circ_0087429 and miR-5003-3p expression in cervical cancer tissue samples. **f.** The colocalization of circ_0087429 and miR-5003-3p in cells was detected by FISH staining. Scale bar, 50 μ m. **g.** The binding sites of circ_0087429 and miR-5003-3p were predicted by circBank. **h-i.** A luciferase reporter assay was used to examine the relative luciferase activity of the circ_0087429WT and circ_0087429MUT. ** $p < 0.01$, *** $p < 0.001$, NS means no statistical significance

lymphatic metastasis compared with non-lymphatic metastasis.

Next, we detected the expression of circ_0087429 in the normal cervical epithelial cell line Ect1/E6E7 and cervical cancer cell lines HeLa, SiHa and CaSki. The expression of circ_0087429 was significantly reduced in cervical

cancer cell lines, and the expression of circ_0087429 was the lowest in HeLa cells (Fig. 1e).

Features and location of circ_0087429

The Sanger sequencing results showed that circ_0087429 originates from the SPIN1 gene located on chromosome

(See figure on next page.)

Fig. 5 The tumour suppressor effect of circ_0087429 in cervical cancer can be reversed by miR-5003-3p. HeLa cells were transfected with pcDNA5.1-NC, pcDNA5.1-circ, pcDNA5.1-circ + mimics NC or pcDNA5.1-circ + miR mimics for subsequent detection. **a-b.** The expression of circ_0087429 and miR-5003-3p in each group was tested by qRT-PCR. **c-g.** CCK-8, EdU and colony formation assays were used to detect the proliferation ability of each group of cells. Scale bar, 50 μ m. **h-i.** Wound healing assays determined the migration ability of each group of cells. Scale bar, 100 μ m. **j-k.** Transwell invasion assays detected the invasion ability of each group of cells. Scale bar, 50 μ m. ** $p < 0.01$, *** $p < 0.001$

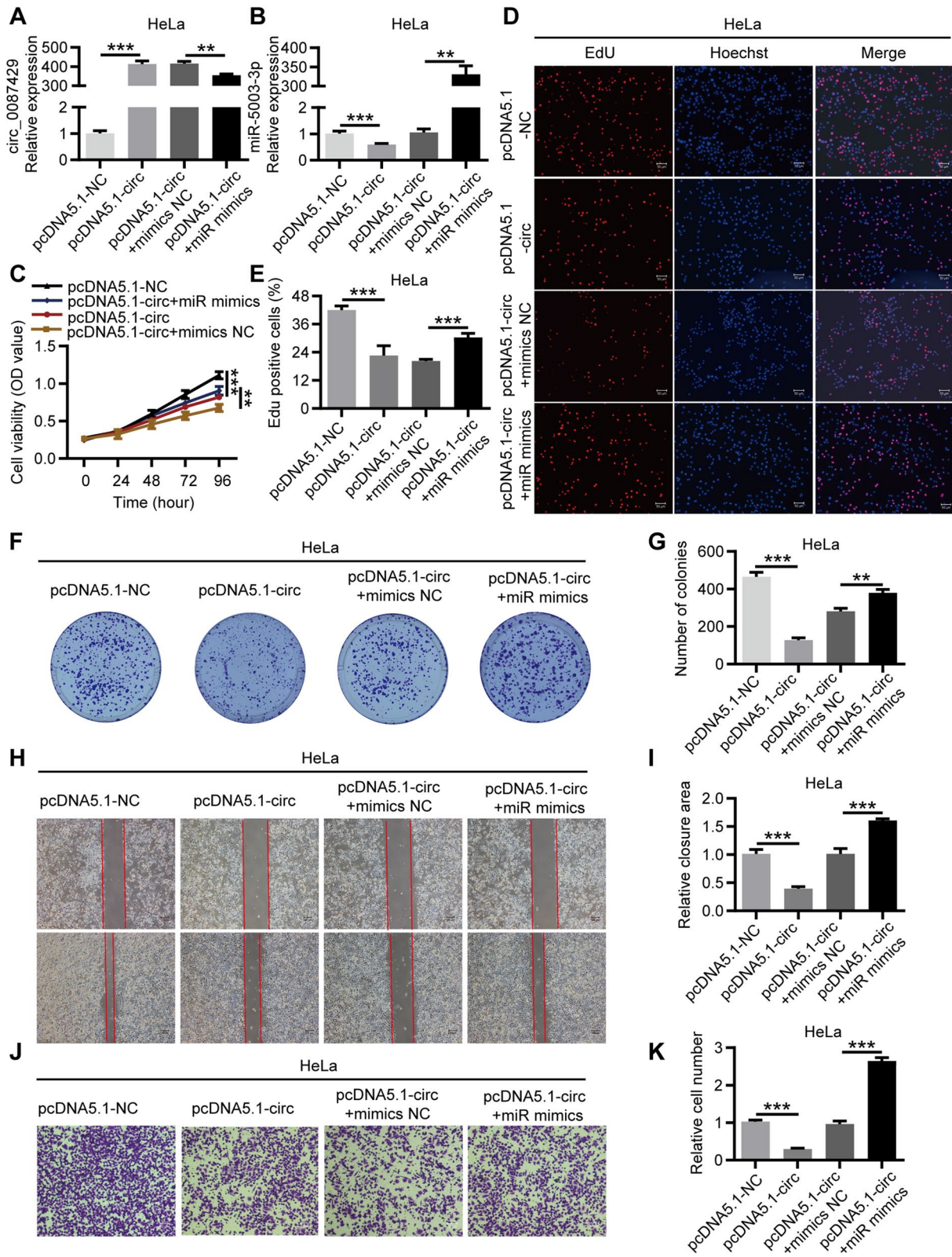


Fig. 5 (See legend on previous page.)

9 and is formed by the splicing of the head and tail of the second exon (Fig. 1f). To further verify the ring structure of circ_0087429, we used RNase R and actinomycin D to verify the stability of circ_0087429. The results showed that compared with SPIN1, circ_0087429 was resistant to RNase R and actinomycin D treatment (Fig. 1g-h). In addition, we detected the cellular location of circ_0087429 by subcellular grade analysis and FISH. We confirmed that circ_0087429 was mainly distributed in the cytoplasm (Fig. 1i-j). The above results indicated that circ_0087429 may be involved in posttranscriptional regulation.

Circ_0087429 inhibits the proliferation, migration, invasion and angiogenesis of cervical cancer in vitro

To explore the biological function of circ_0087429, we constructed an overexpression lentiviral vector for circ_0087429 and established a stable HeLa cell line overexpressing circ_0087429 (Fig. 2a). In addition, three siRNAs targeting circ_0087429 were constructed to knock down circ_0087429 in SiHa cells (Fig. 2b). The results of CCK-8 assays, EdU assays and colony formation assays showed that overexpression of circ_0087429 inhibited the proliferation of cervical cancer cells, while circ_0087429 knockdown promoted their proliferation (Fig. 2c-i). Wound healing and Transwell invasion assays showed that the overexpression of circ_0087429 inhibited the migration and invasion of cervical cancer cells, while circ_0087429 knockdown showed the opposite effects (Fig. 3a-d). HUVEC tube formation experiments showed that when HUVECs were cocultured with cervical cancer cells with circ_0087429 overexpression or knockdown, the tube-forming ability of HUVECs was reduced or enhanced (Fig. 3e-f). To this end, we assessed the expression change of circ_0087429 in HUVECs after coculture, and the results showed that the expression of circ_0087429 in HUVECs increased after coculture with cervical cancer cells overexpressing circ_0087429, and the expression of circ_0087429 decreased after coculture with cervical cancer cells with circ_0087429 knockdown (Fig. 3g). In short, these data suggested that circ_0087429 can inhibit the proliferation, migration and invasion of

cervical cancer cells and alter their angiogenesis ability by affecting the expression of circ_0087429 in peripheral vascular endothelial cells.

Circ_0087429 inhibits the progression of cervical cancer by targeting miR-5003-3p

Current research has shown that circRNAs mainly regulate mRNA expression through competitive binding with miRNAs. Given that circ_0087429 is mainly located in the cytoplasm and exhibits obvious stability, we used the miRNA target prediction tool circBank [23] to predict the potential targets of circ_0087429 and selected 5 candidate miRNAs for further verification. The qRT-PCR results showed that miR-5003-3p was significantly downregulated after overexpression of circ_0087429, and when the expression of circ_0087429 was reduced, the expression of miR-5003-3p was significantly increased (Fig. 4a-b). miR-5003-3p was significantly upregulated in cervical cancer and negatively correlated with the expression of circ_0087429 (Fig. 4c-e). The FISH results showed that miR-5003-3p and circ_0087429 colocalized in the cytoplasm (Fig. 4f). Then, based on the binding sites of circ_0087429 and miR-5003-3p, we constructed circ_0087429-WT and circ_0087429-MUT plasmids. The results of the dual-luciferase reporter assay showed that overexpression of miR-5003-3p significantly reduced the luciferase activity of circ_0087429-WT but did not affect the luciferase activity of circ_0087429-MUT (Fig. 4g-i). These results confirmed that circ_0087429 can interact with miR-5003-3p.

To verify whether circ_0087429 regulates the progression of cervical cancer through miR-5003-3p, we designed rescue experiments. HeLa cells were cotransfected with pcDNA5.1-circ_0087429 and miR-5003-3p mimics, qRT-PCR was used to verify the expression of circ_0087429 and miR-5003-3p after transfection (Fig. 5a-b), and the biological function of each group of cells was evaluated (Fig. 5c-k). Similarly, SiHa cells were cotransfected with si-circ_0087429 and miR-5003-3p inhibitor, and the biological function of each group of cells was evaluated (Fig. S1). The results showed that miR-5003-3p could significantly reverse

(See figure on next page.)

Fig. 6 circ_0087429 downregulates the expression of OGN through competitive binding with miR-5003-3p in cervical cancer. **a.** The databases miRDB, miRWalk, miRDIIP and TargetScan predicted the target genes of miR-5003-3p. **b.** The expression changes in OGN after circ_0087429 overexpression and miR-5003-3p knockdown were determined by qRT-PCR. **c.** The expression changes in OGN after circ_0087429 knockdown and miR-5003-3p overexpression were determined by qRT-PCR. **d.** The expression of OGN was detected by western blotting after the expression of circ_0087429 and miR-5003-3p was changed. **e.** The fluorescence intensity of OGN after circ_0087429 overexpression or knockdown was confirmed by immunofluorescence staining. Scale bar, 25 μ m. **f.** The binding sites of circ_0087429 and miR-5003-3p were predicted by miRWalk. **g.** A luciferase reporter assay was used to examine the relative luciferase activity of OGN-WT and OGN-MUT. **h-i.** The differential expression of OGN between cervical cancer and normal cervical epithelial cell lines was detected by western blotting and qRT-PCR. **j-k.** The differential expression of OGN between cervical cancer (T) and adjacent tissue (P) samples was detected by western blotting and qRT-PCR. **l.** Spearman's correlation analysis confirmed the correlation between circ_0087429 and OGN expression in cervical cancer tissue samples. ** $p < 0.01$, *** $p < 0.001$, NS means no statistical significance

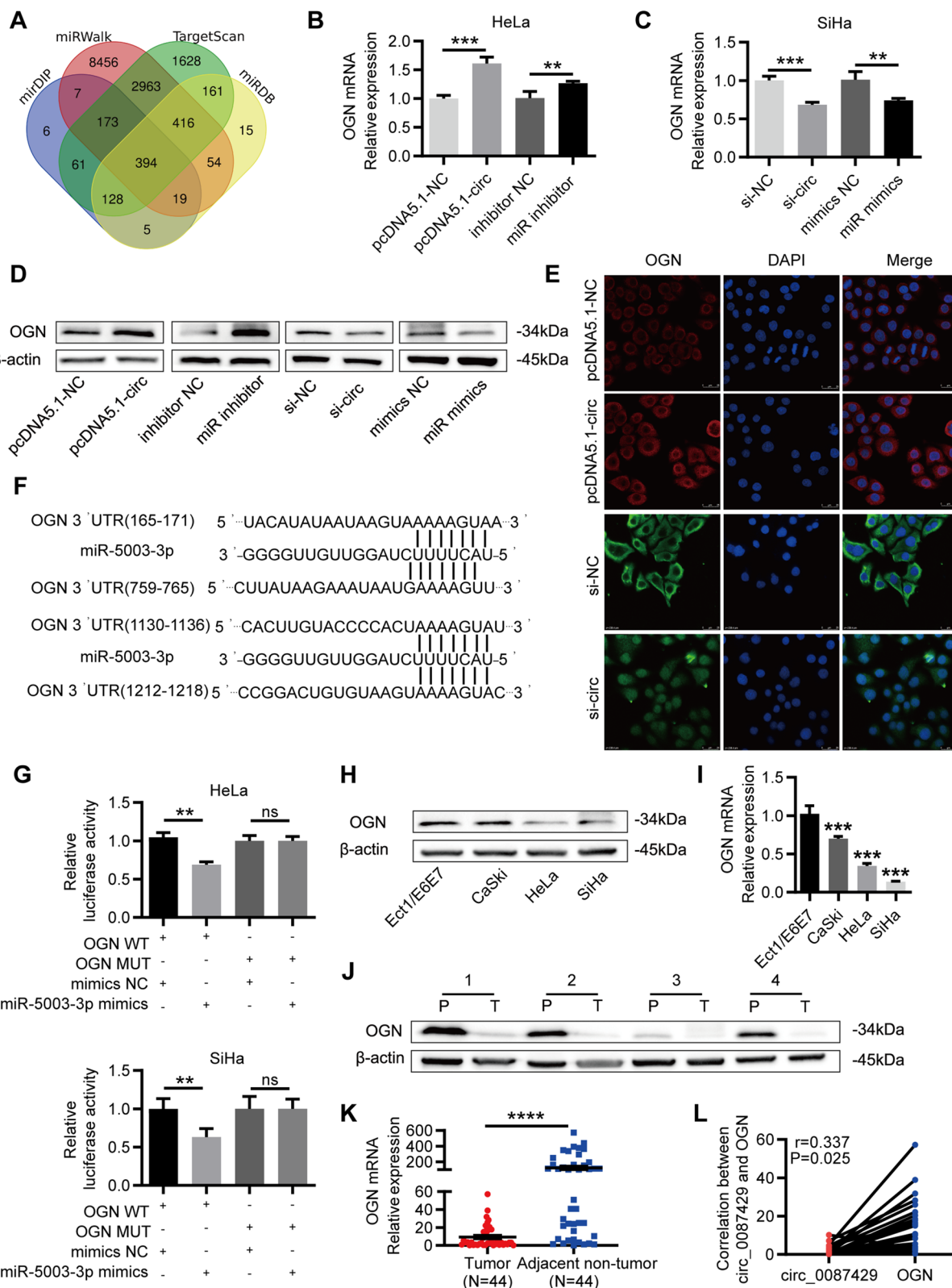


Fig. 6 (See legend on previous page.)

the inhibitory effect of circ_0087429 on the proliferation, migration and invasion of cervical cancer cells. In conclusion, circ_0087429 can inhibit tumour progression by acting as a molecular sponge of miR-5003-3p in cervical cancer.

OGN is a direct target gene of miR-5003-3p and is downregulated in CC

We used the online prediction tools miRDB [24], miR-Walk [25], mirDIP [26] and TargetScan [27] to predict the potential target genes of miR-5003-3p. As shown in the Venn diagram (Fig. 6a), the four databases predicted 394 common target genes. These target genes were crossed with mRNAs that are downregulated by more than fivefold in cervical cancer from The Cancer Genome Atlas (TCGA) database, and 8 target genes were finally obtained (OGN, SCN7A, PGR, PTGER3, FGF7, ADAMTS5, LMO3 and ANK2). Among them, the target gene OGN was the most significantly downregulated in cervical cancer (Fig. S2). Based on the above results, we used qRT-PCR and western blotting to detect the corresponding expression changes in OGN after circ_0087429 and miR-5003-3p expression was altered in cervical cancer cells. The results showed that OGN expression was significantly increased after circ_0087429 overexpression and miR-5003-3p knockdown, while OGN expression was significantly downregulated after circ_0087429 knockdown and miR-5003-3p overexpression (Fig. 6b-d). The results of immunofluorescence staining also showed that the overexpression of circ_0087429 upregulated the expression of OGN, while the expression of OGN decreased correspondingly after circ_0087429 knockdown (Fig. 6e). Then, based on the binding sites of miR-5003-3p and OGN, we constructed OGN-WT and OGN-MUT plasmids. A dual-luciferase reporter assay showed that overexpression of miR-5003-3p significantly reduced the luciferase activity of OGN-WT, while the luciferase activity of OGN-MUT was not affected (Fig. 6f-g). These results indicated that there was a direct interaction between miR-5003-3p and OGN.

It is reported that the expression of OGN is reduced in many different tumours. We assessed the expression of OGN in cervical cancer cells and tissues, and the results confirmed that OGN was significantly downregulated in cervical cancer (Fig. 6h-k). The analysis of the

relationship between OGN and the clinicopathological parameters of cervical cancer patients showed that compared with that in patients with tumours less than 4 cm, the expression of OGN was significantly reduced in cervical cancer patients with larger tumours (Table 1). Correlation analysis showed that the expression levels of OGN and circ_0087429 in cervical cancer tissue were positively correlated (Fig. 6l).

After that, we constructed an overexpression vector of OGN and designed rescue experiments. HeLa cells were co-transfected with miR-5003-3p mimics and OGN overexpression plasmid (Fig. 7a-b), and the biological function of cells in each group was evaluated. The results showed that the promotion on the proliferation, migration and invasion of cervical cancer cells caused by miR-5003-3p mimics could be reversed by OGN overexpression (Fig. 7c-k). Similarly, HeLa cells were cotransfected with pcDNA5.1-circ_0087429 and si-OGN (Fig. S3a-b). The results showed that si-OGN could significantly reverse the inhibitory effect of circ_0087429 on the proliferation, migration and invasion of cervical cancer cells (Fig. S3c-k), indicating that the tumour suppressor effect of circ_0087429 was achieved through the miR-5003-3p/OGN axis.

Circ_0087429 can inhibit EMT in cervical cancer cells through the circ_0087429/miR-5003-3p/OGN axis

It is reported that miR-5003-3p and OGN may participate in the EMT of tumours. To this end, we assessed the effect of circ_0087429 on EMT related proteins. Immunofluorescence staining showed that after circ_0087429 overexpression, the expression of N-cadherin was downregulated, while knockdown of circ_0087429 decreased the expression of E-cadherin (Fig. 8a-b). The western blotting results showed that the overexpression of circ_0087429 increased the expression of E-cadherin, Claudin-1 and decreased the expression of N-cadherin, Vimentin, MMP2 and Snail, while overexpression of miR-5003-3p or knockdown of OGN both reversed the inhibitory effect of circ_0087429 on EMT. In addition, the promotion of EMT after circ_0087429 knockdown could also be reversed by the miR-5003-3p inhibitor, and overexpression of OGN also inhibited the promotion of EMT after miR-5003-3p overexpression (Fig. 8c-d). Therefore, the inhibitory effect of circ_0087429 on EMT is achieved through the circ_0087429/miR-5003-3p/OGN axis.

(See figure on next page.)

Fig. 7 The cancer-promoting effect of miR-5003-3p in cervical cancer can be reversed by OGN. HeLa cells were transfected with mimics NC, miR mimics, miR mimics + oe-NC or miR mimics + oe-OGN for subsequent detection. **a-b**. The expression of miR-5003-3p and OGN in each group was tested by qRT-PCR. **c-g**. CCK-8, EdU and colony formation assays were used to detect the proliferation ability of each group of cells. Scale bar, 50 μ m. **h-i**. Wound healing assays determined the migration ability of each group of cells. Scale bar, 100 μ m. **j-k**. Transwell invasion assays detected the invasion ability of each group of cells. Scale bar, 50 μ m. ****** $p < 0.01$, ******* $p < 0.001$

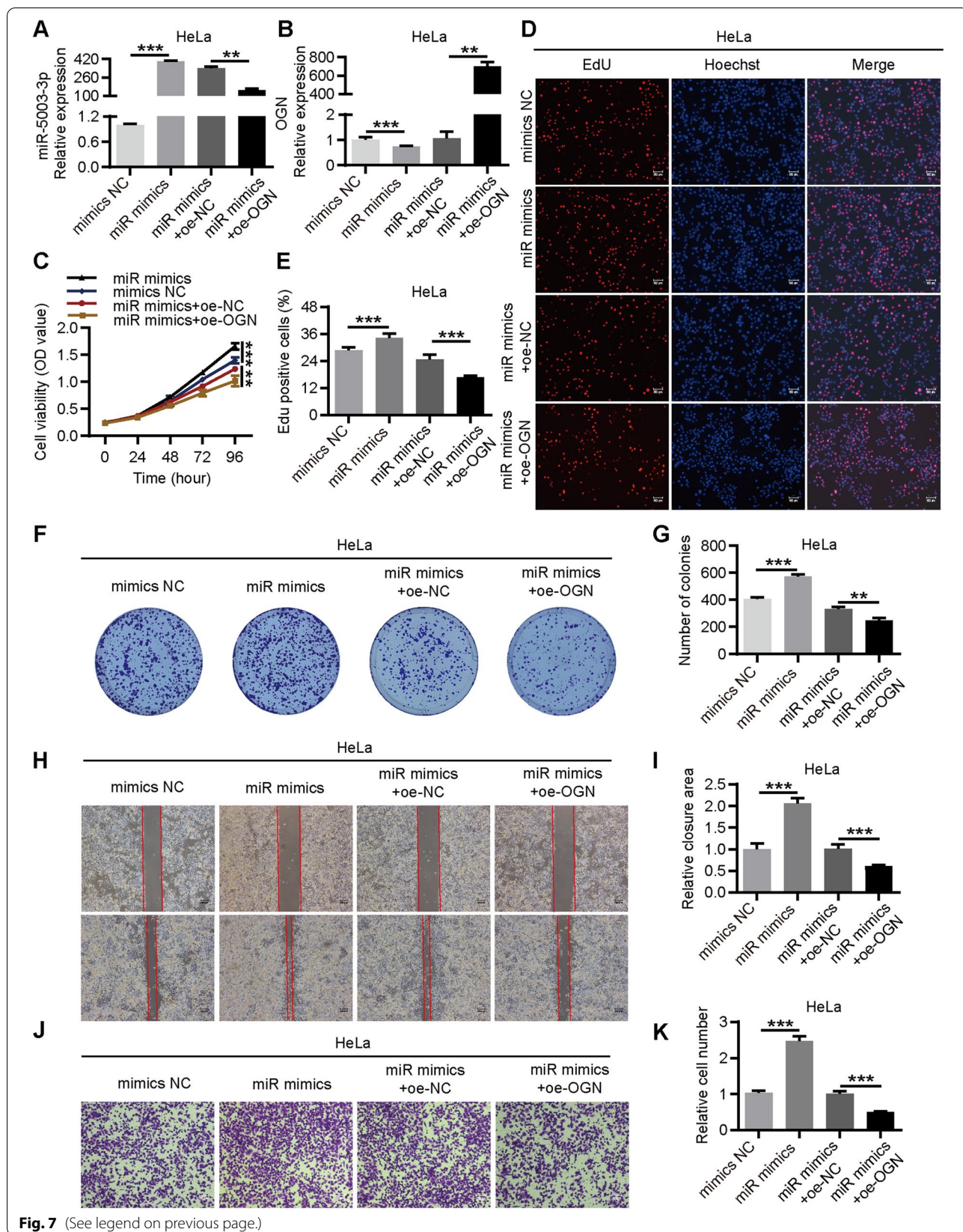


Fig. 7 (See legend on previous page.)

EIF4A3 regulates the expression of circ_0087429

To explore how circ_0087429 is differentially expressed in cervical cancer, we used CircInteractome (<https://circinteractome.nia.nih.gov/>) to predict the RNA binding proteins that match the flanking regions of the circ_0087429, of which EIF4A3 has the most binding sites (Fig. 8e). The results of the RIP assay showed that the parental gene SPIN1 was significantly enriched in the anti-EIF4A3 group compared with the anti-IgG group (Fig. 8f). EIF4A3 was significantly upregulated in cervical cancer (Fig. 8g). After the overexpression of EIF4A3, the expression of circ_0087429 decreased significantly (Fig. 8h-i and 8l). Knockdown of EIF4A3 inhibited the expression of parental gene SPIN1, but significantly promoted the expression of circ_0087429 (Fig. 8j-k and 8m). In conclusion, EIF4A3 can inhibit circ_0087429 expression by binding to its flanking regions.

Overexpression of circ_0087429 in vivo can inhibit the progression of cervical cancer

To further examine the effect of circ_0087429 on tumour growth in animal models, we subcutaneously injected HeLa cells stably transfected with pcDNA5.1-NC or pcDNA5.1-circ_0087429 into BALB/c nude mice. Tumour size was measured every 7 days, and the mice were sacrificed after four weeks. The results showed that the tumour volume and weight were significantly reduced after circ_0087429 overexpression (Fig. 9a-c). The qRT-PCR results of subcutaneous tumour tissues showed that the expression of miR-5003-3p was downregulated after the overexpression of circ_0087429, while the expression of OGN was upregulated (Fig. 9d). The western blotting and immunohistochemical staining results showed that the expression of OGN and E-cadherin was increased, and the expression of N-cadherin was decreased in tumour tissues overexpressing circ_0087429. In addition, the expression of CD31 and Ki67 decreased in tumour tissues overexpressing circ_0087429 (Fig. 9e-h). In order to investigate the effect of circ_0087429 on tumour metastasis, we injected HeLa cells stably transfected with pcDNA5.1-NC or pcDNA5.1-circ_0087429 into nude mice through the tail vein. The results showed that the circ_0087429 overexpression group had fewer lung and liver metastatic nodules (Fig. 9i-l).

In summary, EIF4A3-downregulated circ_0087429 is a tumour suppressor gene that can promote the expression of OGN and inhibit the EMT of cervical cancer cells by competitively binding miR-5003-3p (Fig. 9m).

Discussion

As a noncoding RNA, circRNAs are highly expressed, stable in structure, and able to survive in a complex microenvironment. They are considered to be key regulators of the occurrence and development of cancer [28]. In cervical cancer, some circRNAs with cancer-promoting effects, such as circTPCN [13] and other circRNAs with anticancer effects, such as circTPCN, have been reported [29]. However, the role of most circRNAs in the development of cervical cancer remains unexplored, and these circRNAs may provide new targets for clarifying the pathogenesis and refining the clinical treatment of cervical cancer [30]. In this study, we found that an unknown circRNA, circ_0087429, was significantly downregulated in cervical cancer. And circ_0087429 was closely related to the International Federation of Gynecology and Obstetrics (FIGO) stage and lymphatic metastasis of cervical cancer patients.

Based on this phenomenon, we explored the possible role and mechanism of circ_0087429 in cervical cancer. The results of functional experiments showed that circ_0087429 can significantly inhibit the proliferation, migration, invasion and angiogenesis of cervical cancer. The ceRNA mechanism is an important mechanism by which circRNAs function. The circRNAs in the cytoplasm can bind to miRNAs and inhibit their functions, thereby releasing downstream target genes from miRNA-mediated inhibition, highlight their roles as miRNA sponges [31]. This study first verified the ring structure of circ_0087429 and clarified its cellular location, which indicated that circ_0087429 could be involved in posttranscriptional regulation. After that, we used bioinformatics methods to screen out miR-5003-3p, which has a complementary sequence to circ_0087429, and a target gene of miR-5003-3p (OGN). qRT-PCR verified the correlations between the three genes. A dual-luciferase reporter assay was

(See figure on next page.)

Fig. 8 EIF4A3-regulated circ_0087429 can inhibit EMT in cervical cancer cells through the circ_0087429/miR-5003-3p/OGN axis. **a-b.**

Immunofluorescence staining detected the fluorescence intensities of N-cadherin or E-cadherin upon circ_0087429 overexpression or knockdown, respectively. Scale bar, 25 μ m. **c-d.** EMT related proteins in each group of cells were detected by western blotting. **e.** The binding sites for EIF4A3 in the flanking sequences of the SPIN1 mRNA transcript were predicted using CircInteractome. **f.** RIP assay demonstrated the binding between SPIN1 and EIF4A3. **g.** The differential expression of EIF4A3 between cervical cancer and normal cervical epithelial cell lines was detected by western blotting. **h-i.** The expression of EIF4A3 in the two groups of SiHa cells of oe-NC and oe-EIF4A3 was detected by qRT-PCR and western blotting. **j-k.** The expression of EIF4A3 in Caski cells treated with siRNA was detected by qRT-PCR and western blotting. **l.** The expression of circ_0087429 and EIF4A3 in SiHa cells stably overexpressing EIF4A3 were detected by qRT-PCR. **m.** The expression of circ_0087429 and EIF4A3 in Caski cells treated with si-EIF4A3 were detected by qRT-PCR. * $p < 0.05$, ** $p < 0.01$, **** $p < 0.0001$

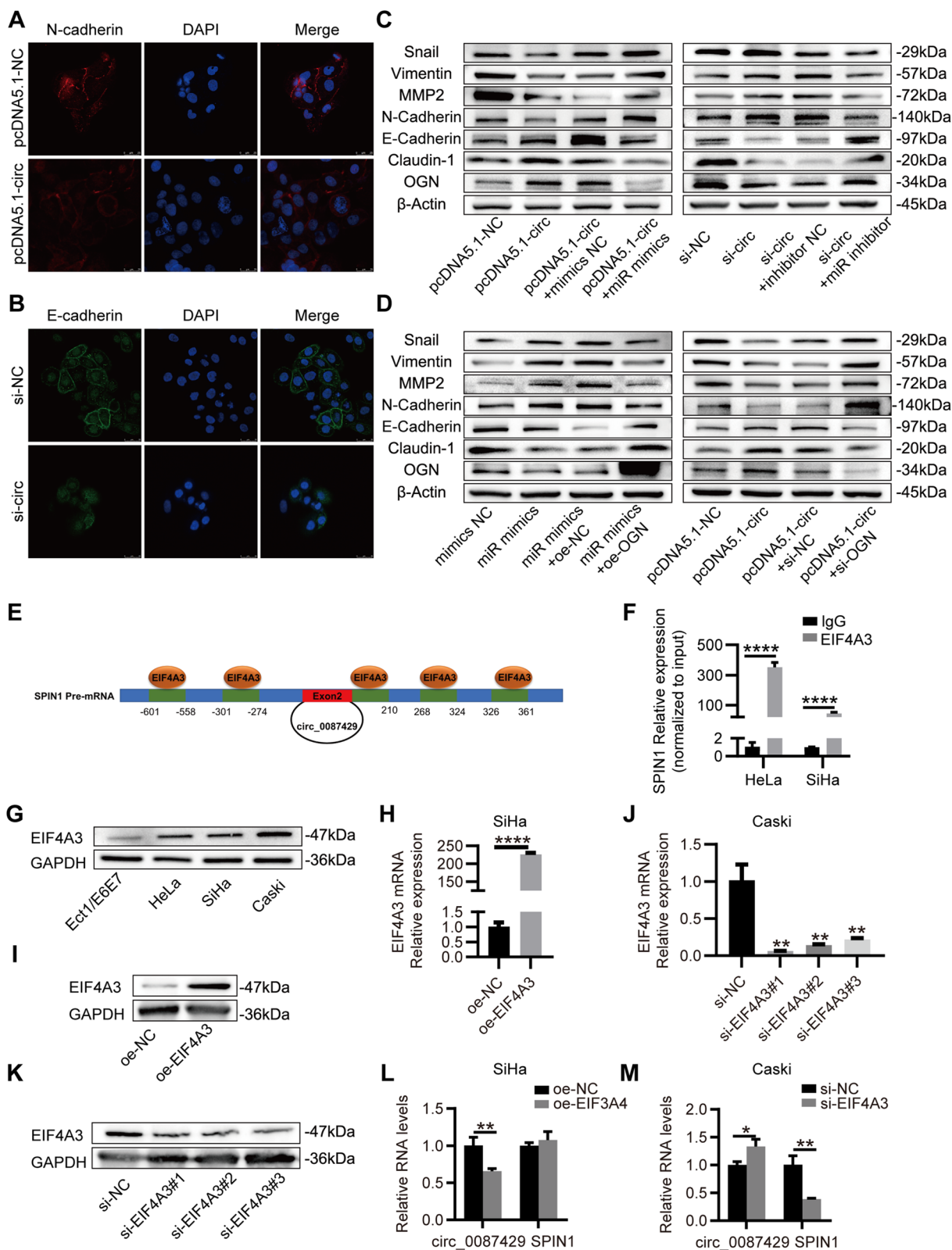


Fig. 8 (See legend on previous page.)

applied to verify the interactions between circ_0087429 and miR-5003-3p and between miR-5003-3p and OGN. The role of miR-5003-3p and OGN in cervical cancer is still unknown. This study verified the tumour-promoting effect of miR-5003-3p in cervical cancer for the first time and confirmed that it can block the tumour-suppressive effect of circ_0087429. Later, it was verified that OGN expression is downregulated in cervical cancer and is closely related to tumour size in cervical cancer patients. Functional experiments showed that OGN has a tumour-suppressive effect, the tumour-promoting effect of miR-5003-3p in cervical cancer can be inhibited by the target gene OGN, and downregulation of OGN can also block the tumour-suppressive effect of circ_0087429. The above results suggest that the tumour-suppressive effect of circ_0087429 in cervical cancer is achieved through the circ_0087429/miR-5003-3p/OGN axis.

EMT is the process by which quiescent epithelial cells transform into mesenchymal-phenotype cells. Cancer cells have plasticity and can continuously adapt to the constantly changing tumour microenvironment, and this process is mediated by EMT [32]. In addition, EMT is involved in cancer cell stemness regulation, metabolic reprogramming, treatment resistance, immune escape and other biological processes [33–35]. Studies have shown that miR-5003-3p in breast cancer can promote the stability of snail, and then promote tumour metastasis through EMT [17]. OGN can reverse EMT through the PI3K/Akt/mTOR pathway in breast cancer [22], and reduce the expression of ZEB-1 through the EGFR/Akt signaling pathway in colon cancer to inhibit EMT [21]. Given that both miR-5003-3p and OGN participate in EMT of tumours, we explored the influence of circ_0087429 on the EMT in cervical cancer. The results showed that circ_0087429 can inhibit EMT, and the inhibitory effect can be achieved through the circ_0087429/miR-5003-3p/OGN axis.

The exon junction complex (EJC) is deposited by spliceosomes onto mRNAs at 20–24 nucleotides upstream of exon-exon junctions, where it serves as a molecular marker for the correct splicing of precursor mRNA [36]. EIF4A3 is the core component of EJC, which can

be used as RNA binding protein to play an important role by participating in mRNA splicing and influencing its downstream events such as transport and translation [37]. circRNAs are produced by alternative splicing [38]. Studies have reported that EIF4A3 can affect the expression level of circRNA by participating in the back-splicing of circRNA [39]. For example, EIF4A3 can be combined with the flanking sequence of circMMP9 to promote the expression of circMMP9 [40]. EIF4A3 is upregulated in various malignant tumours such as pancreatic cancer, breast cancer and cervical cancer [41–43]. In this study, we confirmed the binding of EIF4A3 to SPIN1 by RIP assay, and verified the expression changes of circ_0087429 and its parent gene SPIN1 after overexpression and knockdown of EIF4A3. In conclusion, EIF4A3 can inhibit circ_0087429 expression by binding to SPIN1 and affecting its cyclization. EIF4A3 plays a significant role in the induction and maintenance of stress granules [44]. The formation of stress granules provides the basis for tumours to exhibit an aggressive phenotype and drug resistance [45]. Accumulation of stress granules can also induce metabolic changes in cancer cells and promote tumour growth [46, 47]. It has been reported that circRNAs can participate in the formation of stress granules [48], while circRNAs play important roles in cancer metastasis, drug resistance and regulation of cancer cell metabolism [6, 49]. Does circ_0087429 play a role in the formation of stress granules in cancer cells? Can it participate in the metastasis, metabolism and drug resistance of cancer cells by regulating the formation of stress granules? These questions are all worthy of further exploration.

Conclusions

In summary, our research shows that there is a new tumour suppressor gene, circ_0087429, in cervical cancer; circ_0087429 can regulate the expression of its target gene OGN by competitively binding with miR-5003-3p, thereby inhibiting EMT in the occurrence and development of cancer. EIF4A3 can inhibit its expression by binding to the flanking regions of circ_0087429. Our findings provide a new potential target for the treatment of cervical cancer.

(See figure on next page.)

Fig. 9 Overexpression of circ_0087429 in vivo can inhibit the progression of cervical cancer **a.** Image of subcutaneous tumour tissues in the circ_0087429-overexpressing group and control group. **b-c.** Volume and weight of subcutaneous tumour tissues in each group. **d.** The expression levels of circ_0087429, miR-5003-3p and OGN in subcutaneous tumour tissues of each group were detected by qRT-PCR. **e-f.** The expression levels of OGN, N-cadherin and E-cadherin in subcutaneous tumour tissues of each group were detected by western blotting. **g-h.** The expression levels of OGN, N-cadherin, E-cadherin, Ki67 and CD31 in subcutaneous tumour tissues of each group were detected by immunohistochemical staining. Scale bar, 30 μ m. **i-l.** Representative images and bar graphs of liver (i-) and lung (k-) metastases with circ_0087429-overexpressing group and control group in a nude mouse metastatic tumour model. Metastatic nodules are indicated by arrows. Scale bar, 60 μ m. **m.** A schematic diagram showing how circ_0087429 regulates the expression of OGN by sponging miR-5003-3p and thereby reverses EMT. MET: mesenchymal to epithelial transition. * $p < 0.05$, ** $p < 0.01$, *** $p < 0.001$

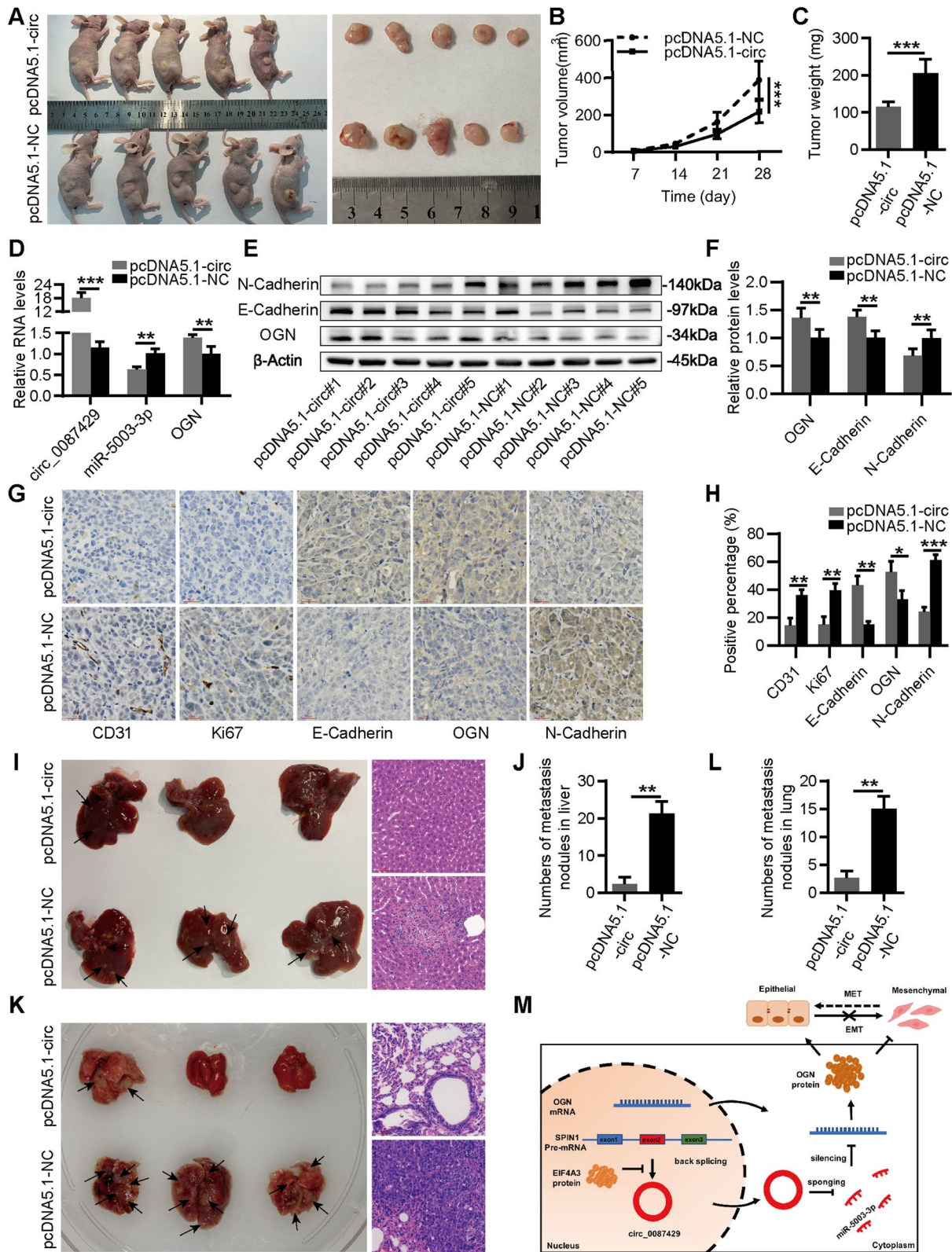


Fig. 9 (See legend on previous page.)

Abbreviations

circRNA: Circular RNA; GEO: Gene Expression Omnibus; ceRNA: Competitive endogenous RNA; miRNA: MicroRNA; EMT: Epithelial to mesenchymal transition; SLRPs: Small leucine-rich proteoglycans; OGN: Osteoglycin; EIF4A3: Eukaryotic initiation factor 4A-III; qRT-PCR: Quantitative real-time polymerase reaction; FISH: Fluorescence in situ hybridization; CCK-8: Cell Counting Kit-8; Edu: 5-Ethynyl-20-deoxyuridine; IF: Immunofluorescence; IHC: Immunohistochemistry; SD: Standard deviation; FIGO: Federation International of Gynecology and Obstetrics; HPV: Human papilloma virus; TCGA: The Cancer Genome Atlas; ATCC: American Type Culture Collection; H&E: Hematoxylin and eosin; GEPIA: Gene Expression Profiling Interactive Analysis; EJC: Exon junction complex; RIP: RNA immunoprecipitation.

Supplementary Information

The online version contains supplementary material available at <https://doi.org/10.1186/s13046-022-02368-4>.

Additional file 1: Table S1. Primers used in this study. **Table S2.** Oligonucleotides used in this study. **Additional file 2: Fig. S1** The cancer-promoting effect of si-circ_0087429 in cervical cancer can be reversed by the miR-5003-3p inhibitor. SiHa cells were transfected with si-NC, si-circ, si-circ + inhibitor NC or si-circ + miR inhibitor for subsequent detection. a-b. The expression of circ_0087429 and miR-5003-3p in each group was tested by qRT-PCR. c-g. CCK-8, Edu and colony formation assays were used to detect the proliferation ability of each group of cells. Scale bar, 50 μ m. h-i. Wound healing assays were used to determine the migration ability of each group of cells. Scale bar, 100 μ m. j-k. Transwell invasion assays were used to detect the invasion ability of each group of cells. Scale bar, 50 μ m. **Additional file 3: Fig. S2** The expression of 8 target genes in cervical tissues based on the GEPIA database. a. OGN, b. SCN7A, c. PGR, d. PTGER3, e. FGF7, f. ADAMTS5, g. LMO3, h. ANK2. **Additional file 4: Fig. S3** The tumour suppressor effect of circ_0087429 in cervical cancer can be reversed by si-OGN. HeLa cells were transfected with pcDNA5.1-NC, pcDNA5.1-circ, pcDNA5.1-circ + si-NC or pcDNA5.1-circ + si-OGN for subsequent detection. a-b. The expression of circ_0087429 and OGN in each group was tested by qRT-PCR. c-g. CCK-8, Edu and colony formation assays were used to detect the proliferation ability of each group of cells. Scale bar, 50 μ m. h-i. Wound healing assays were used to determine the migration ability of each group of cells. Scale bar, 100 μ m. j-k. Transwell invasion assays were used to detect the invasion ability of each group of cells. Scale bar, 50 μ m. ******** $p < 0.0001$

Acknowledgements

Not applicable.

Authors' contributions

MQY and LFH designed this study. MQY and FL performed the experiments. JYD and BY performed the data analysis and designed the figures. BYH and HRH reviewed the clinical data. MQY and SFW wrote the draft of the manuscript. LFH and XQG revised the manuscript. The author(s) read and approved the final manuscript.

Funding

This study was supported by the grant from the National Science Foundation of China (NO. 81572546, 81972422 and 81771529).

Availability of data and materials

The datasets used and/or analysed during the current study are available from the corresponding author on reasonable request.

Declarations

Ethics approval and consent to participate

All the clinical experiments in this study were approved by the Ethics Committee of the Shanghai First Maternity and Infant Hospital. All the included

patients signed an informed consent form. All animal care and experiments were approved by the Animal Care Committee of Tongji University.

Consent for publication

Not applicable.

Competing interests

The authors declare that they have no competing interests.

Author details

¹Department of Gynecology, Shanghai First Maternity and Infant Hospital, School of Medicine, Tongji University, Shanghai 200092, China. ²Department of Gynecology, Shanghai East Hospital, School of Medicine, Tongji University, Shanghai 200120, China. ³Department of Obstetrics and Gynecology, Shanghai General Hospital, Shanghai Jiao Tong University School of Medicine, Shanghai 201620, China. ⁴Department of Gynecology, the First Affiliated Hospital of Wenzhou Medical University, Wenzhou, Zhejiang 325027, China.

Author details

¹Department of Gynecology, Shanghai First Maternity and Infant Hospital, School of Medicine, Tongji University, Shanghai 200092, China. ²Department of Obstetrics and Gynecology, Shanghai General Hospital, Shanghai Jiao Tong University School of Medicine, Shanghai 201620, China. ³Department of Gynecology, the First Affiliated Hospital of Wenzhou Medical University, Wenzhou, Zhejiang 325027, China. ⁴Department of Gynecology, Shanghai East Hospital, School of Medicine, Tongji University, Shanghai 200120, China.

Received: 13 December 2021 Accepted: 19 April 2022

Published online: 05 May 2022

References

- Kalliala I, Athanasiou A, Veroniki AA, Salanti G, Efthimiou O, Raftis N, Bowden S, Paraskevas M, Aro K, Arbyn M, et al. Incidence and mortality from cervical cancer and other malignancies after treatment of cervical intraepithelial neoplasia: a systematic review and meta-analysis of the literature. *Ann Oncol*. 2020;31(2):213–27.
- Sung H, Ferlay J, Siegel RL, Laversanne M, Soerjomataram I, Jemal A, Bray F. Global Cancer Statistics 2020: GLOBOCAN Estimates of Incidence and Mortality Worldwide for 36 Cancers in 185 Countries. *CA: a cancer journal for clinicians*. 2021;71(3):209–49.
- Simms KT, Hanley SJB, Smith MA, Keane A, Canfell K. Impact of HPV vaccine hesitancy on cervical cancer in Japan: a modelling study. *The Lancet Public health*. 2020;5(4):e223–34.
- Kristensen LS, Andersen MS, Stagsted LW, Ebbesen KK, Hansen TB, Kjems J. The biogenesis, biology and characterization of circular RNAs. *Nat Rev Genet*. 2019;20(11):675–91.
- Li H, Xu JD, Fang XH, Zhu JN, Yang J, Pan R, Yuan SJ, Zeng N, Yang ZZ, Yang H, et al. Circular RNA circRNA_000203 aggravates cardiac hypertrophy via suppressing miR-26b-5p and miR-140-3p binding to Gata4. *Cardiovasc Res*. 2020;116(7):1323–34.
- Yu T, Wang Y, Fan Y, Fang N, Wang T, Xu T, Shu Y. Circular RNAs in cancer metabolism: a review. *J Hematol Oncol*. 2019;12(1):90.
- Shen S, Yang Y, Shen P, Ma J, Fang B, Wang Q, Wang K, Shi P, Fan S, Fang X. circPDE4B prevents articular cartilage degeneration and promotes repair by acting as a scaffold for RIC8A and MID1. *Ann Rheum Dis*. 2021;80(9):1209–19.
- Chen LL. The expanding regulatory mechanisms and cellular functions of circular RNAs. *Nat Rev Mol Cell Biol*. 2020;21(8):475–90.
- He L, Man C, Xiang S, Yao L, Wang X, Fan Y. Circular RNAs' cap-independent translation protein and its roles in carcinomas. *Mol Cancer*. 2021;20(1):119.
- Vo JN, Cieslik M, Zhang Y, Shukla S, Xiao L, Zhang Y, Wu YM, Dhanasekaran SM, Engelke CG, Cao X, et al. The Landscape of Circular RNA in Cancer. *Cell*. 2019;176(4):869–881.e813.
- Rong Z, Shi S, Tan Z, Xu J, Meng Q, Hua J, Liu J, Zhang B, Wang W, Yu X, et al. Circular RNA CircEYA3 induces energy production to promote pancreatic ductal adenocarcinoma progression through the miR-1294/c-Myc axis. *Mol Cancer*. 2021;20(1):106.

12. Luo Z, Rong Z, Zhang J, Zhu Z, Yu Z, Li T, Fu Z, Qiu Z, Huang C. Circular RNA circCCDC9 acts as a miR-6792-3p sponge to suppress the progression of gastric cancer through regulating CAV1 expression. *Mol Cancer*. 2020;19(1):86.
13. Tian-Zhao D, Yang Y, Xing-Xuan W, Yu-Xin C, Xue-Lian W. Profiling of circular RNAs and circTPCN/miR-634/mTOR regulatory pathway in cervical cancer. *Genomics*. 2021;113(4):2253–63.
14. Zhou M, Yang Z, Wang D, Chen P, Zhang Y. The circular RNA circZFR phosphorylates Rb promoting cervical cancer progression by regulating the SSBP1/CDK2/cyclin E1 complex. *J Exp Clin Cancer Res*. 2021;40(1):48.
15. Mohajeri M, Banach M, Atkin SL, Butler AE, Ruscica M, Watts GF, Sahebkar A. MicroRNAs: Novel Molecular Targets and Response Modulators of Statin Therapy. *Trends Pharmacol Sci*. 2018;39(11):967–81.
16. Rzepiela AJ, Ghosh S, Breda J, Vina-Vilaseca A, Syed AP, Gruber AJ, Eschbach K, Beisel C, van Nimwegen E, Zavolan M. Single-cell mRNA profiling reveals the hierarchical response of miRNA targets to miRNA induction. *Mol Syst Biol*. 2018;14(8):e2266.
17. Kwak SY, Yoo JO, An HJ, Bae IH, Park MJ, Kim J, Han YH. miR-5003-3p promotes epithelial-mesenchymal transition in breast cancer cells through Snail stabilization and direct targeting of E-cadherin. *J Mol Cell Biol*. 2016;8(5):372–83.
18. Appunni S, Anand V, Khandelwal M, Gupta N, Rubens M, Sharma A. Small Leucine Rich Proteoglycans (decorin, biglycan and lumican) in cancer. *Clinica chimica acta; international journal of clinical chemistry*. 2019;491:1–7.
19. Pietraszek-Gremplewicz K, Karamanou K, Niang A, Dauchez M, Belloy N, Maquart FX, Baud S, Brézillon S. Small leucine-rich proteoglycans and matrix metalloproteinase-14: Key partners? *Matrix biology : journal of the International Society for Matrix Biology*. 2019;75–76:271–85.
20. Lomnytska MI, Becker S, Hellman K, Hellström AC, Souchelnyskiy S, Mints M, Hellman U, Andersson S, Auer G. Diagnostic protein marker patterns in squamous cervical cancer. *Proteomics Clin Appl*. 2010;4(1):17–31.
21. Hu X, Li YQ, Li QG, Ma YL, Peng JJ, Cai SJ. Osteoglycin (OGN) reverses epithelial to mesenchymal transition and invasiveness in colorectal cancer via EGFR/Akt pathway. *J Exp Clin Cancer Res*. 2018;37(1):41.
22. Xu T, Zhang R, Dong M, Zhang Z, Li H, Zhan C, Li X. Osteoglycin (OGN) Inhibits Cell Proliferation and Invasiveness in Breast Cancer via PI3K/Akt/mTOR Signaling Pathway. *Onco Targets Ther*. 2019;12:10639–50.
23. Liu M, Wang Q, Shen J, Yang BB, Ding X. Circbank: a comprehensive database for circRNA with standard nomenclature. *RNA Biol*. 2019;16(7):899–905.
24. Chen Y, Wang X. miRDB: an online database for prediction of functional microRNA targets. *Nucleic Acids Res*. 2020;48(D1):D127–d131.
25. Dweep H, Sticht C, Pandey P, Gretz N. miRWalk–database: prediction of possible miRNA binding sites by “walking” the genes of three genomes. *J Biomed Inform*. 2011;44(5):839–47.
26. Tokar T, Pastrello C, Rossos AEM, Abovsky M, Hauschild AC, Tsay M, Lu R, Jurisica I. mirDIP 4.1-integrative database of human microRNA target predictions. *Nucleic Acids Res*. 2018;46(D1):D360–d370.
27. Agarwal V, Bell GW, Nam JW, Bartel DP. Predicting effective microRNA target sites in mammalian mRNAs. *Elife*. 2015;4.
28. Kristensen LS, Hansen TB, Venø MT, Kjems J. Circular RNAs in cancer: opportunities and challenges in the field. *Oncogene*. 2018;37(5):555–65.
29. Xu J, Zhang Y, Huang Y, Dong X, Xiang Z, Zou J, Wu L, Lu W. circEYA1 Functions as a Sponge of miR-582-3p to Suppress Cervical Adenocarcinoma Tumorigenesis via Upregulating CXCL14. *Mol Ther Nucleic Acids*. 2020;22:1176–90.
30. Shen H, Liu B, Xu J, Zhang B, Wang Y, Shi L, Cai X. Circular RNAs: characteristics, biogenesis, mechanisms and functions in liver cancer. *J Hematol Oncol*. 2021;14(1):134.
31. Lu Q, Liu T, Feng H, Yang R, Zhao X, Chen W, Jiang B, Qin H, Guo X, Liu M, et al. Circular RNA circSLC8A1 acts as a sponge of miR-130b/miR-494 in suppressing bladder cancer progression via regulating PTEN. *Mol Cancer*. 2019;18(1):111.
32. Tulchinsky E, Demidov O, Kriajevska M, Barlev NA, Imyanov E. EMT: A mechanism for escape from EGFR-targeted therapy in lung cancer. *Biochim Biophys Acta*. 2019;1871(1):29–39.
33. Bai F, Zhang LH, Liu X, Wang C, Zheng C, Sun J, Li M, Zhu WG, Pei XH. GATA3 functions downstream of BRCA1 to suppress EMT in breast cancer. *Theranostics*. 2021;11(17):8218–33.
34. Pan G, Liu Y, Shang L, Zhou F, Yang S. EMT-associated microRNAs and their roles in cancer stemness and drug resistance. *Cancer communications (London, England)*. 2021;41(3):199–217.
35. Ramesh V, Brabletz T, Ceppi P. Targeting EMT in Cancer with Repurposed Metabolic Inhibitors. *Trends in cancer*. 2020;6(11):942–50.
36. Ye J, She X, Liu Z, He Z, Gao X, Lu L, Liang R, Lin Y. Eukaryotic Initiation Factor 4A–3: A Review of Its Physiological Role and Involvement in Oncogenesis. *Front Oncol*. 2021;11: 712045.
37. Kanellis DC, Espinoza JA, Zisi A, Sakkas E, Bartkova J, Katsori AM, Boström J, Dyrskjöt L, Broholm H, Altun M, et al. The exon-junction complex helicase eIF4A3 controls cell fate via coordinated regulation of ribosome biogenesis and translational output. *Science advances*. 2021;7(32).
38. S L, Genetics SJJN. Detecting circular RNAs: bioinformatic and experimental challenges. *Nat Rev Genet*. 2016;17(11):679–92.
39. Zheng S, Huang M, Xing L, Yang R, Wang X, Jiang R, Zhang L, Chen J. The circRNA circSEPT9 mediated by E2F1 and EIF4A3 facilitates the carcinogenesis and development of triple-negative breast cancer. *Mol Cancer*. 2020;19(1):73.
40. Wang R, Zhang S, Chen X, Li N, Li J, Jia R, Pan Y, Liang H. EIF4A3-induced circular RNA MMP9 (circMMP9) acts as a sponge of miR-124 and promotes glioblastoma multiforme cell tumorigenesis. *Mol Cancer*. 2018;17(1):166.
41. Meznad K, Paget-Bailly P, Jacquin E, Peigney A, Aubin F, Guittaut M, Mouglin C, Prétet JL, Baguet A. The exon junction complex core factor eIF4A3 is a key regulator of HPV16 gene expression. *Biochemical reports*. 2021;41(4).
42. Xu Y, Zhang S, Liao X, Li M, Chen S, Li X, Wu X, Yang M, Tang M, Hu Y, et al. Circular RNA circIKBKB promotes breast cancer bone metastasis through sustaining NF-κB/bone remodeling factors signaling. *Mol Cancer*. 2021;20(1):98.
43. Li Q, Lei C, Lu C, Wang J, Gao M, Gao W. LINC01232 exerts oncogenic activities in pancreatic adenocarcinoma via regulation of TM95F2. *Cell Death Dis*. 2019;10(10):698.
44. Mazloomian A, Araki S, Ohori M, El-Naggar AM, Yap D, Bashashati A, Nakao S, Sorensen PH, Nakanishi A, Shah S, et al. Pharmacological systems analysis defines EIF4A3 functions in cell-cycle and RNA stress granule formation. *Communications biology*. 2019;2:165.
45. Shi Q, Zhu Y, Ma J, Chang K, Ding D, Bai Y, Gao K, Zhang P, Mo R, Feng K, et al. Prostate Cancer-associated SPOP mutations enhance cancer cell survival and docetaxel resistance by upregulating Caprin1-dependent stress granule assembly. *Mol Cancer*. 2019;18(1):170.
46. Mukhopadhyay S, Vander Heiden MG, McCormick F. The Metabolic Landscape of RAS-Driven Cancers from biology to therapy. *Nature cancer*. 2021;2(3):271–83.
47. Protter DSW, Parker R. Principles and Properties of Stress Granules. *Trends Cell Biol*. 2016;26(9):668–79.
48. Chen S, Zhang J, Zhao F. Screening Linear and Circular RNA Transcripts from Stress Granules. *Genomics, proteomics & bioinformatics*. 2022.
49. Xu J, Ji L, Liang Y, Wan Z, Zheng W, Song X, Gorshkov K, Sun Q, Lin H, Zheng X, et al. CircRNA-SORE mediates sorafenib resistance in hepatocellular carcinoma by stabilizing YBX1. *Signal Transduct Target Ther*. 2020;5(1):298.

Publisher's Note

Springer Nature remains neutral with regard to jurisdictional claims in published maps and institutional affiliations.

Ready to submit your research? Choose BMC and benefit from:

- fast, convenient online submission
- thorough peer review by experienced researchers in your field
- rapid publication on acceptance
- support for research data, including large and complex data types
- gold Open Access which fosters wider collaboration and increased citations
- maximum visibility for your research: over 100M website views per year

At BMC, research is always in progress.

Learn more biomedcentral.com/submissions

